Distribution Agreement

In presenting this thesis or dissertation as a partial fulfillment of the requirements for an advanced degree from Emory University, I hereby grant to Emory University and its agents the non-exclusive license to archive, make accessible, and display my thesis or dissertation in whole or in part in all forms of media, now or hereafter known, including display on the world wide web. I understand that I may select some access restrictions as part of the online submission of this thesis or dissertation. I retain all ownership rights to the copyright of the thesis or dissertation. I also retain the right to use in future works (such as articles or books) all or part of this thesis or dissertation.

Signature:

_____ _____

Nicole Ando Date

.

Synthesis, Characterization, and Dioxygen Reactivity of a Copper(I) Complex Supported by a Tripodal Tetraamine Ligand

By
Nicole Ando

Master of Science

Chemistry

_____
Cora MacBeth, Ph.D.
Advisor

_____
Karl Hagen, Ph.D.
Committee Member

_____
Chris Scarborough, Ph.D.
Committee Member

Accepted:

_____
Lisa A. Tedesco, Ph.D.
Dean of the James T. Laney School of Graduate Studies

_____ Date

Synthesis, Characterization, and Dioxygen Reactivity of a Copper(I) Complex Supported by a Tripodal Tetraamine Ligand

By

Nicole Ando
B.S., James Madison University, 2010

Advisor: Cora MacBeth, Ph.D.

An abstract of
A thesis submitted to the Faculty of the
James T. Laney School of Graduate Studies of Emory University
in partial fulfillment of the requirements for the degree of Master of Science in Chemistry
2012

Abstract

Synthesis, Characterization, and Dioxygen Reactivity of a Copper(I) Complex Supported by a Tripodal Tetraamine Ligand

By Nicole Ando

In this manuscript, the tripodal tetradentate ligand tris(2-dimethylaminophenyl)amine (L^{Me}) has been prepared and shown to be less electron donating than the other commonly employed tetradentate ligands tris(N,N-dimethylaminoethyl)amine (Me_6tren) and tris(2-pyridylmethyl)amine (tmpa). The ligand L^{Me} can be metallated with a copper(I) source to yield the corresponding mononuclear complex, $[Cu^{I}(L^{Me})(CH_3CN)]PF_6$. When $[Cu^{I}(L^{Me})(CH_3CN)]PF_6$ is exposed to dioxygen in a solution of acetone at low temperature (-78 ^{o}C), it readily reacts to produce a dicopper(II) *trans*-μ-1,2-peroxo complex, $[Cu^{II}_2(L^{Me})_2(\mu\text{-}1,2\text{-}O_2)](PF_6)_2$. This complex has been characterized by resonance Raman and UV-visible absorption spectroscopies and is compared to predeceasing dicopper(II) *trans*-μ-1,2-peroxo complexes. The decayed product of $[Cu^{II}_2(L^{Me})_2(\mu\text{-}1,2\text{-}O_2)](PF_6)_2$ has been isolated and characterized as he mononuclear terminal hydroxide complex $[Cu^{II}(L^{Me})(OH)]PF_6$. The reactivity of $[Cu^{II}_2(L^{Me})_2(\mu\text{-}1,2\text{-}O_2)](PF_6)$ towards the aerobic oxidation of toluene to benzaldehyde is also described.

Synthesis, Characterization, and Dioxygen Reactivity of a Copper(I) Complex Supported by a Tripodal Tetraamine Ligand

By

Nicole Ando
B.S., James Madison University, 2010

Advisor: Cora MacBeth, Ph.D.

A thesis submitted to the Faculty of the
James T. Laney School of Graduate Studies of Emory University
in partial fulfillment of the requirements for the degree of Master of Science in Chemistry
2012

Table of Contents

List of Figures, Tables, Charts, and Schemes

Schemes

List of Abbreviations

BDE	Bond dissociation energy
pMMO	Particulate methane monooxygenase
THF	Tetrahydrofuran
Me_6tren	Tris(N,N'-dimethylaminoethyl)amine
tmpa	Tris(2-pyridylmethyl)amine
L^{Me}	N(*o*-$PhNMe_2)_3$, tris(2-dimethylaminophenyl)amine
PF_6	Hexafluorophosphate
OTf	Triflate, Trifluoromethanesulfonate
$NaBPh_4$	Sodium tetraphenylborate

I. Introduction

The oxidation of hydrocarbons remains a challenge in chemistry due to the high bond dissociation energies (BDEs) of C—H bonds (i.e., 85-105 kcal/mol) and the high kinetic barrier associated with this reaction.[1] Common oxidation reactions employed in fine chemical syntheses require the use of stoichiometric amounts of inorganic oxidants like chromates and permanganates.[2] Although these transformations work well, they yield stoichiometric amounts of inorganic byproduct along with the oxidized organic product. This feature of these reactions will often prevent their use in large-scale industrial processes.

Using dioxygen as an oxidant in catalytic oxidation reactions is appealing because it is inexpensive, abundant, and its byproducts are environmentally benign. Several important industrial processes in industry use dioxygen as an oxidant. The Wacker process, for example, uses a palladium catalyst with a copper co-catalyst to facilitate the oxidation of terminal alkenes to aldehydes.[3,4] One of the drawbacks associated with this process is the relative expense associated with palladium, a second-row coinage metal. The other limitation associated with this process is the required regeneration of the palladium catalyst by the copper co-catalyst, which inhibits productivity and selectivity. To advance the field of catalytic aerobic oxidation, new, robust catalysts that incorporate inexpensive, abundant, first-row transition metals must be developed.

In biology, a wide variety of metalloenzymes utilize dioxygen as a terminal oxidant to perform selective substrate oxidations that proceed under mild conditions.[5-7] The active sites of metallo-enzymes that carry out oxidation reactions typically incorporate earth abundant transition metal ions, such as iron and copper. These metal

ions have several accessible oxidation states and their reduced forms readily react with dioxygen. Monooxygenases are a class of metalloenzymes that incorporate one oxygen atom, derived from dioxygen, into the substrate. One type of monooxygenase that has attracted a great deal of attention is the particulate methane monooxygenases (pMMO), due to its unique ability to hydroxylate methane, a hydrocarbon substrate with a very strong C—H BDE (ca. 104 kcal mol^{-1}).[6,8,9] The crystal structure of pMMO obtained by Rosenzweig and co-workers reveals both monocopper and dicopper sites within the enzyme where dioxygen reactivity is believed to occur.[6,8,10] However, the resolution of the crystal structure (2.5 Å) leaves some room for interpretation and endorses the use of alternative methods to gather information about the active site of the enzyme responsible for its unique reactivity.

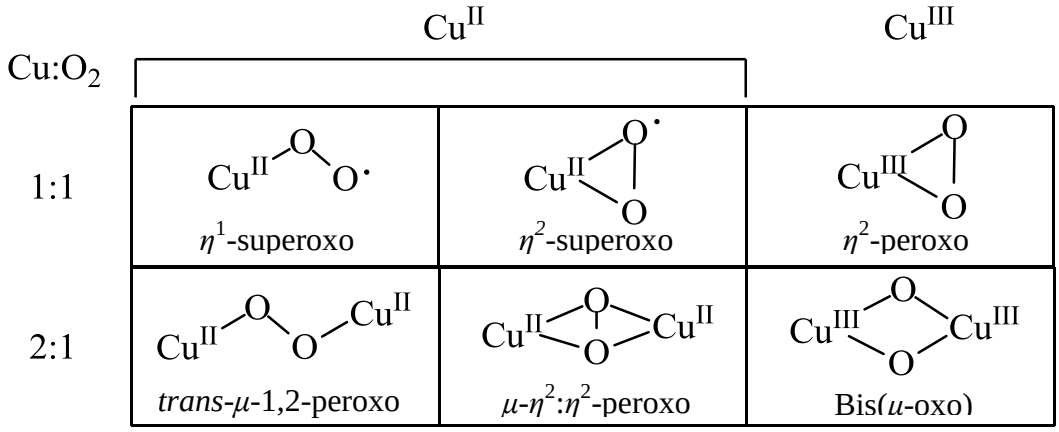

Figure 1. Possible copper-dioxygen binding modes resulting from the reaction of copper(I) with dioxygen.

A number of seminal biomimetic studies have furthered our understanding of the dioxygen binding modes that are operative in biological processes.[5,11-13] One possibility is that of dioxygen binding to a single metal ion. When a one-electron oxidation of the

metal ion occurs with concurrent reduction of dioxygen to superoxide, an end-on (η^1-superoxide) or side-on (η^2-superoxide) can be formed.[14-18] Another possible mononuclear conformation is a side-on peroxide structure (η^2-peroxo), which forms when the metal ion is oxidized by two electrons.[19-21] A mononuclear copper-dioxygen species, specifically a Cu(II)-η^1-superoxide complex, is believed to be the reactive intermediate in both peptidylglycine α-hydroxylating monooxygenase and dopamine β-monooxygenase.[7,11-13,22-24] However, in synthetic systems, Cu(II)-η^1-superoxide species are often difficult to isolate because, once formed, they further react with an additional copper(I) complex in solution to form a dinuclear copper complex with bridging peroxo or μ-oxo ligands.[25-29] Therefore, the bridging peroxo binding modes have been observed more frequently in synthetic biomimetic complexes than the mononuclear η^1-superoxo binding modes. These complexes can form in an end-on (*trans*-μ-1,2-peroxo) or side-on (μ-η^2:η^2-peroxo) fashion. Examples of biological systems that react with dioxygen to form copper species with bridging peroxo ligands include hemocyanin and tyrosinase. These systems both bind dioxygen in a side-on μ-η^2:η^2-peroxo fashion.[8,28,22,12] The various copper to dioxygen binding modes illustrated in **Figure 1** have all been well characterized by various spectroscopic techniques including UV-visible absorption and resonance Raman spectroscopies. Each specific binding mode gives rise to its own set of unique spectroscopic characteristics.[30]

Synthetic copper-dioxygen complexes have exhibited a wide variety of reactivity. For example, Itoh and co-workers reported a copper-η^1-superoxide complex that can facilitate the intraligand oxidation of a phenol to a quinone.[31] Karlin and co-workers have reported a dicopper complex that exists in solution in equilibrium between the μ-

η^2:η^2-peroxo and bis(μ-oxo) forms that is capable of hydroxylating THF and oxidatively *N*-dealkylating exogenous substrates.[32,33] Stack has reported tyrosinase-like reactivity of dinuclear-μ-η^2:η^2-peroxo complexes towards phenolates to produce catechols and quinones.[34,35] Nam, Karlin, and Fukuzumi have also recently demonstrated that both a dicopper-μ-η^2:η^2-peroxo complex and dicopper-bis(μ-oxo) complexes can also be used to catalytically reduce dioxygen to water.[36,37] These studies have included a detailed discussion of the possible mechanisms for this reaction. They concluded that the supporting ligand influences the complexes' internal reorganizational energy during catalysis, supporting different mechanistic pathways.

In recent work, Karlin and Schindler separately showed that copper(I) complexes supported by chelating tetraamine ligands could be reacted with dioxygen to generate dicopper complexes containing a *trans*-μ-1,2-peroxo ligand (i.e., $[Cu_2L_2(\mu\text{-}1,2\text{-}O_2)]^{2+}$, where L = a tetradentate ligand). Furthermore, their detailed studies demonstrated that these $[Cu_2L_2(\mu\text{-}1,2\text{-}O_2)]^{2+}$ species could be used in the stoichiometric oxidation of toluene to benzaldehyde.[38,39] Some of the tripodal tetraamine ligands used in these studies are shown in **Figure 2**. These chelating ligand scaffolds play an important role in regulating the dioxygen reactivity by their corresponding copper(I) complexes.

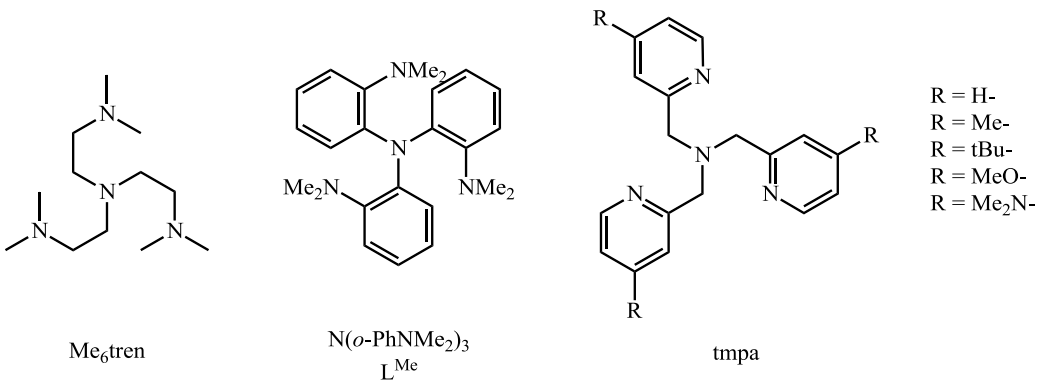

Figure 2. Tripodal tetraamine ligands.

Tripodal tetraamine ligands have been studied for copper coordination chemistry, because of their ability to provide a nitrogen rich coordination sphere similar to the histidine rich coordination environment found in copper-containing metalloproteins. These ligand scaffolds can typically be metallated with copper(I) precursors to form complexes with trigonal pyramidal coordination geometries. This coordination geometry allows for open coordination sites available for dioxygen reactivity.[27,40] To elucidate the electronic effects of the resulting copper-dioxygen complexes, Zhang and co-workers synthesized a series of complexes that varied in the substituent of the *para* position of tris(2-pyridylmethyl)amine (tmpa) (**Figure 2**). This work demonstrated that stronger electron donating ligands could be used to enhance the thermal stability of a dicopper-μ-1,2-peroxo species derived from dioxygen.[25] Based on these studies, we have chosen to focus on a ligand previously reported by our lab, tris(2-dimethylaminophenyl)amine, (L^{Me}).[41,42] This ligand, seen in **Figure 2**, incorporates a phenyl into the backbone of the chelating rings, enhancing its rigidity and differentiating L^{Me} from previously studied tripodal tetradentate ligands by Karlin and Schindler.[38,39] This report will discuss L^{Me} as

a complex of copper(I), the complex's ability to bind dioxygen, and its subsequent reactivity towards the oxidation of toluene.

II. Results and discussion

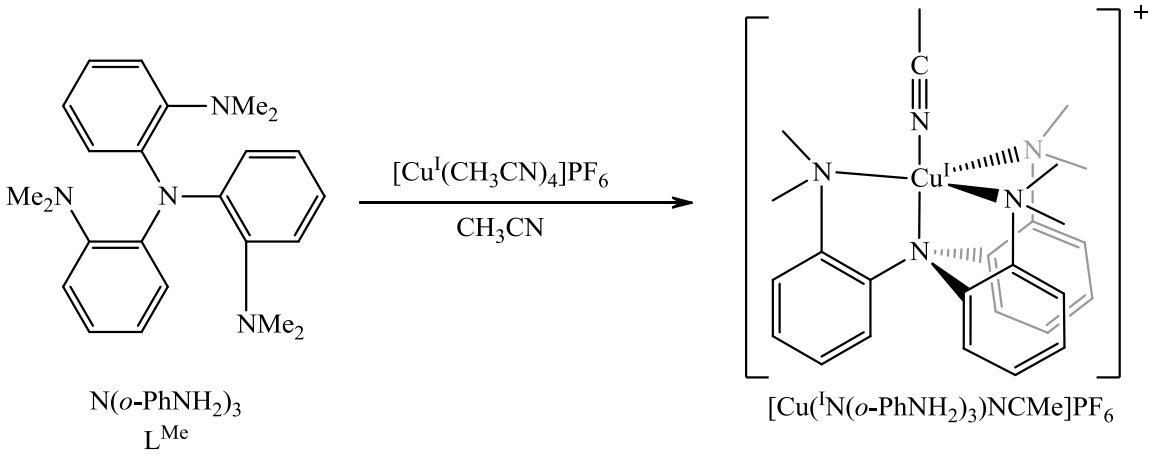

Scheme 1. Metallation of the ligand, L^{Me}, with $[Cu^{I}(CH_3CN)_4]PF_6$ to produce $[Cu^{I}(L^{Me})(CH_3CN)]PF_6$.

Synthesis and Characterization of Cu^{I} Complexes. The ligand, L^{Me}, was synthesized in good yields using a literature procedure previously reported by our lab.[42,43] The metallation of L^{Me} with Cu^{I} (**Scheme 1**) can be achieved using modified literature procedures with either acetonitrile or acetone as the solvent.[38,41] Difficulties arose upon dissolving the complex, $[Cu^{I}(L^{Me})(CH_3CN)]PF_6$, in acetone and similar polar organic solvents. Disproportionation occurred, forming a red precipitate (copper metal) and a yellow solution. This problem has previously been reported and can be minimized by the use of fresh starting material and a change in counterions.[28,44] Therefore, the $Cu^{I}(L^{Me})(OTf)$ complex was synthesized using a modified literature procedure.[39] Both complexes, $[Cu^{I}(L^{Me})(CH_3CN)]PF_6$ and $Cu^{I}(L^{Me})(OTf)$, were characterized using infrared and ^{1}H NMR spectroscopies, as well as mass spectrometry. The crystal structures of $[Cu^{I}(L^{Me})(CH_3CN)]PF_6$ and $Cu^{I}(L^{Me})(OTf)$ (**Figure 3**) have been obtained by the diffusion of ether into an acetone solution. These studies show that all four nitrogens of

L^{Me} are coordinating to the copper center in both of these copper(I) complexes. Both complexes exhibit a distorted trigonal bipyramidal coordination geometry with the axial site occupied by either an acetonitrile solvent molecule in $[Cu^{I}(L^{Me})(CH_3CN)]PF_6$ or the triflate anion in $Cu^{I}(L^{Me})(OTf)$. Since the $Cu^{I}(L^{Me})(OTf)$ complex replaces the solvent molecule with the counterion, this complex remains stable in polar organic solvents, unlike its $[Cu^{I}(L^{Me})(CH_3CN)]PF_6$ counterpart (**Figure 3**).

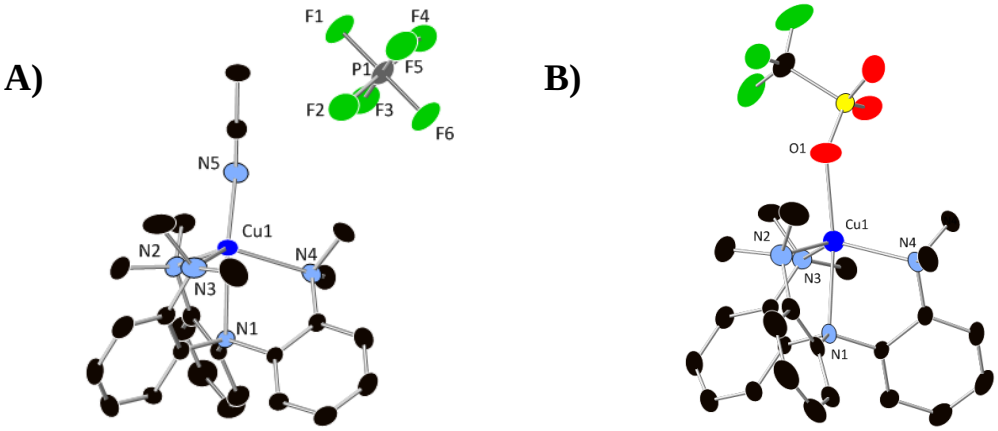

Figure 3. Crystal structures of Cu(I) complexes of L^{Me} (thermal ellipsoid plots drawn at 50% probability) of **(A)** $[Cu^{I}(L^{Me})(CH_3CN)]PF_6$ and **(B)** $Cu^{I}(L^{Me})(OTf)$. Hydrogen atoms are omitted for clarity.

Table 1. Selected metrical parameters of (**A**) and (**B**).

Bond lengths/angles (Å / °)	**$[Cu^{I}(L^{Me})(CH_3CN)]PF_6$**	**$Cu^{I}(L^{Me})(OTf)$**
Cu1—N1	2.36(2)	2.30(2)
Ave. Cu1—N(2,3,4)	2.44(2)	2.17(2)
Cu1—N5/O1	1.95(3)	2.22(2)
N1—Cu1—N(2,3,4)	75.5(8)	78.37(8)
N1—Cu1—N5/O1	174.6(10)	170.23(8)

Electronic Studies of the Ligand N(*o*-PhNMe$_2$)$_3$ (L^{Me}). To investigate the relative ligand field strength of L^{Me}, the copper(II) complex $[Cu^{II}(L^{Me})Cl]PF_6$ was synthesized. This complex has been completely characterized by a variety of spectroscopic and structural methods. The complex was analyzed by UV-visible absorption spectroscopy and its spectrum was directly compared to the closely related Cu(II)-chloride complexes of tmpa and Me_6tren (i.e., $[Cu^{II}(tmpa)Cl]PF_6$ and $[Cu^{II}(Me_6tren)Cl]PF_6$).[41,44,45] All three complexes exhibit two d-d absorption bands in their UV-visible absorption spectra, as summarized in **Table 2.** This absorption pattern, a low-energy transition followed by a higher energy transition with lower intensity absorption, is characteristic of the trigonal bipyramidal geometry of the copper(II) complex being maintained in solution.[30] Since all three complexes maintain the same geometry, it is possible to determine the relative field strength of the ligands by comparing the low-energy d-d transition of the complexes. These data strongly suggest

that Me_6tren (932 nm) is the strongest-field ligand because the $[Cu^{II}(Me_6tren)Cl]ClO_4$ species gives rise to the most blue-shifted spectrum.

Table 2. UV-visible absorption data for the halogenated complexes of Me_6tren, tmpa, and L^{Me} with corresponding molar absorptivity values.

Complex	**Wavelengths (nm)**	**Molar absorptivities ($M^{-1}cm^{-1}$)**
$[Cu^{II}(Me_6tren)Cl]ClO_4$ [a]	740, 932	187, 440
$[Cu^{II}(tmpa)Cl]PF_6$ [b]	632^{sh}, 962	90, 210
$[Cu^{II}(L^{Me})Cl]PF_6$ [c]	782, 1033	146, 306

[a] Ref 3. [b] Ref 5. [c] Ref 1.

To further evaluate the electron donating nature of these ligands, the carbonyl stretching frequencies (ν_{CO}) of the corresponding Cu(I)-carbonyl complexes ($[Cu^{I}(Me_6tren)CO]PF_6$, $[Cu^{I}(tmpa)CO]PF_6$, and $[Cu^{I}(L^{Me})CO]PF_6$) were analyzed by infrared spectroscopy. This approach can also be used to probe potential differences in ligand coordination modes by exploring differences in the complexes' solution and solid-state infrared spectra.[39,41,46,47] The data summarized in **Table 3** shows that $[Cu^{I}(tmpa)CO]PF_6$ and $[Cu^{I}(L^{Me})CO]PF_6$ exhibit similar spectroscopic trends. The lowest ν_{CO} observed for both complexes (2077 and 2088 cm^{-1}) is observed in their solid-state (nujol spectra), where both species exist exclusively as five-coordinate complexes. The shift to higher frequencies (2090 and 2094 cm^{-1}) observed for both of these species in THF suggest that these two complexes exist in equilibrium between five-coordinate and four-coordinate species in solution. The relatively high value for the nujol carbonyl

stretch of $[Cu^{I}(Me_6tren)CO]PF_6$ suggests that in the solid-state this complex exists exclusively as a four-coordinate species.[41,48-51] We postulate that value of the ν_{CO} decreases significantly in the solution-state IR spectrum of $[Cu^{I}(Me_6tren)CO]PF_6$ as the five-coordinate species becomes accessible through a solution state equilibrium. The trend of the carbonyl stretches suggest that L^{Me} is a weaker electron donating ligand than tmpa because the carbonyl stretching frequency for $[Cu^{I}(L^{Me})CO]PF_6$ is higher, indicating less electron density is donated into the anti-bonding π^*-orbital of the coordinated carbonyl ligand.

Table 3. Infrared data for the carbonyl stretching frequency in Cu(I) complexes of Me_6tren, tmpa, and L^{Me} for both Nujol and solution state in THF.

Complex	**ν_{CO} (cm^{-1}) nujol**	**ν_{CO} (cm^{-1}) THF**
$[Cu^{I}(Me_6tren)CO]PF_6$ [a]	2098	2078
$[Cu^{I}(tmpa)CO]PF_6$ [b]	2077	2090
$[Cu^{I}(L^{Me})CO]PF_6$ [a]	2088	2094

[a] Ref 1. [b] Ref 6.

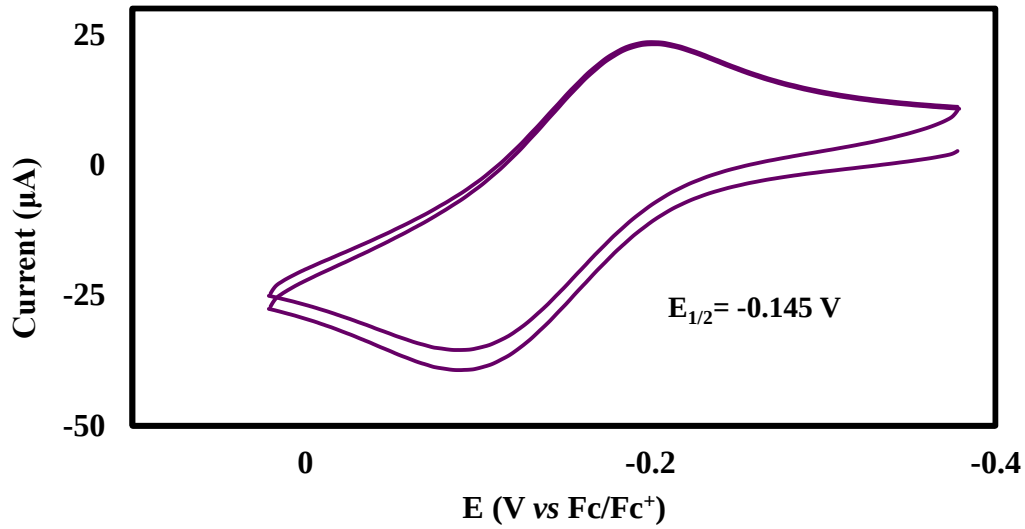

Figure 4. Cyclic voltammogram of $[Cu^{I}(L^{Me})(CH_3CN)]PF_6$ in acetone with 0.1 M tetrabutylammonium hexafluorophosphate ($TBAPF_6$) as the supporting electrolyte at 100mV/sec. Corrected vs. Fc/Fc^+ couple, $E_{1/2}$ = -0.145 V, ΔE = 0.112 V, i_{pa}/i_{pc} = 1.92.

To further explore the nature of the ligand bound to the copper center, electrochemical studies were performed. Cyclic voltammogram of $[Cu^{I}(L^{Me})(CH_3CN)]^+$ measured in acetone displays a quasi-reversible event occurring at -0.145 V (when corrected vs. Fc/Fc^+) as seen in **Figure 4**. The redox potential for $[Cu^{I}(tmpa)(CH_3CN)]^+$ has been reported as -0.01 V vs. SCE in acetonitrile by Kitagawa and co-workers.[44] To compare the two complexes, Kitagawa's redox potential is converted to correct against Fc/Fc^+ using values reported by Connelly and Geiger.[52] This converted value is -0.41 V vs. Fc/Fc^+. Although a trend cannot necessarily be establish, the more positive redox potential shift of $[Cu^{I}(L^{Me})(CH_3CN)]^+$ indicates a greater stabilization of the copper(I) oxidation state compared to $[Cu^{I}(tmpa)(CH_3CN)]^+$. The electrochemical data is consistent with the electronic studies of tripodal tetraamine ligands suggesting our ligand L^{Me} is relatively the weakest field ligand.

Reactivity of Cu^{I} Complexes Binding with Dioxygen. To probe the reactivity of $[Cu^{I}(L^{Me})(CH_3CN)]PF_6$ and $Cu^{I}(L^{Me})(OTf)$ with dioxygen, low temperature oxygenation experiments were conducted. At low temperatures (-78 ^{o}C), both $[Cu^{I}(L^{Me})(CH_3CN)]PF_6$ and $Cu^{I}(L^{Me})(OTf)$ form light yellow solutions when dissolved in acetone and react immediately with dioxygen to form a deep blue solution. The blue species is unstable in solution upon warming to room temperature and decomposes to a mononuclear copper(II) terminal hydroxide, which will be discussed later. When excess diethyl ether is added to the blue species in solution at low temperature, the complex can be precipitated as a microcrystalline blue powder, which can be isolated by filtration. This blue solid is stable at room temperature and can be stored in air for weeks without any visible sign of decomposition.

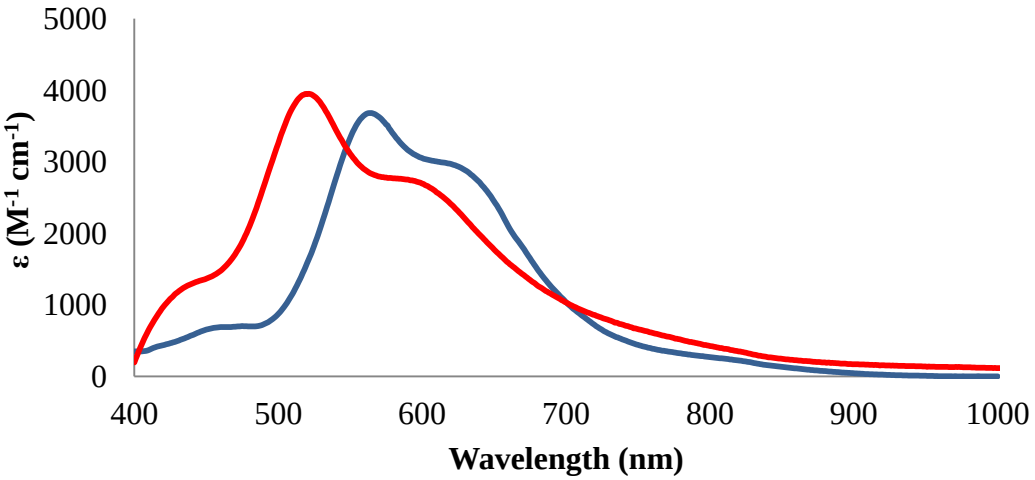

Figure 5. UV-visible absorption spectra of $[Cu^{II}_2(L^{Me})_2(\mu\text{-}1,2\text{-}O_2)](PF_6)_2$ (Blue) and $[Cu^{II}_2(tmpa)_2(\mu\text{-}1,2\text{-}O_2)](BPh_4)_2$ (Red) generated in-situ through a reaction of the corresponding Cu(I) complexes with O_2(g) low temperature, -75 ^{o}C in acetone.

X-ray quality single crystals of the blue oxygenated compound have not yet been isolated, but the complex has been characterized by UV-visible absorption and resonance Raman spectroscopies. These spectroscopic studies strongly suggest the majority of the species formed upon oxygenation is the end-on bridging peroxide species, $[Cu^{II}_2(L^{Me})_2(\mu\text{-}1,2\text{-}O_2)]^{2+}$. The low temperature UV-visible absorption spectrum (**Figure 5**) of $[Cu^{II}_2(L^{Me})_2(\mu\text{-}1,2\text{-}O_2)]^{2+}$ exhibits two absorption bands at 564 nm (3681 $M^{-1}\,cm^{-1}$), and a shoulder at 614 nm (2991 $M^{-1}\,cm^{-1}$). To show a direct comparison between our complex and previously synthesized complexes, $[Cu^{I}(tmpa)(CH_3CN)]BPh_4$ was synthesized and the UV-visible absorption spectrum is shown in **Figure 5**. The spectroscopic pattern observed in both complexes show a lower energy, higher intensity peak followed by a higher energy, lower intensity peak. This is consistent with the literature reports of dicopper complexes with a *trans*-μ-1,2-peroxo ligand, like $[Cu(tmpa)(CH_3CN)]BPh_4$ as well as $[Cu^{I}(Me_6tren)]BPh_4$.[30,53] The intense bands are attributed to LMCT bands arising from $\pi_\sigma^* \rightarrow$ d and $\pi_v^* \rightarrow$ d electron transfers.[30]

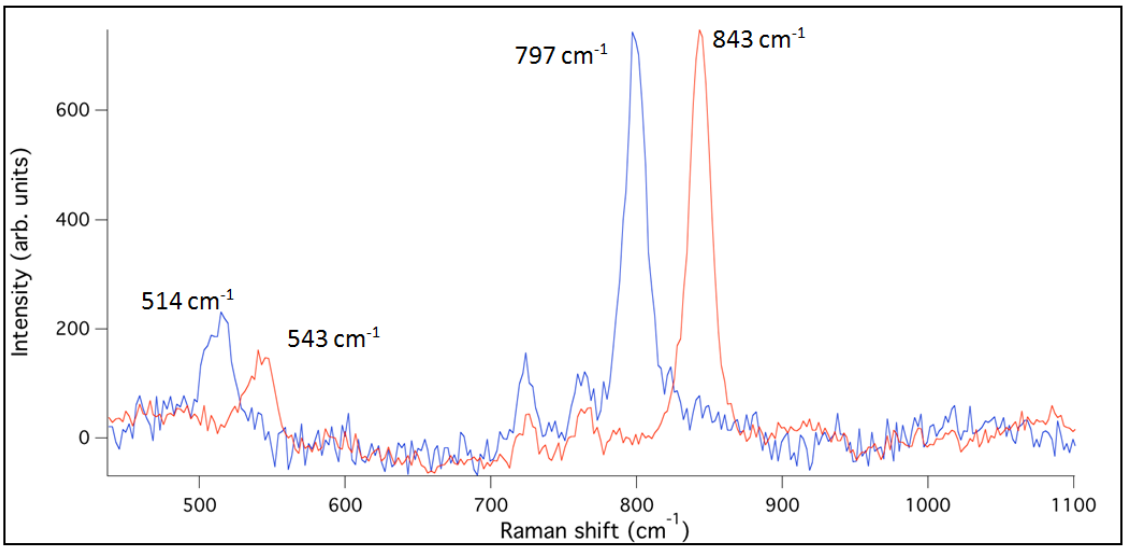

Figure 6. Solid state resonance Raman at 514 nm excitation of $[Cu_2(L^{Me})_2(^{16}O_2)]^{2+}$ (red) and the ^{18}O labeling (blue).

The binding mode of the peroxide ligand in $[Cu_2(L^{Me})_2(\mu\text{-}1,2\text{-}O_2)]^{2+}$ has been confirmed by solid-state resonance Raman spectroscopy (**Figure 6**). A peak at 843 cm^{-1} is observed and is assigned to the oxygen-oxygen bond in dicopper(II)-end-on peroxo complexes. This value is consistent with the data reported for both $[Cu_2(tmpa)_2(\mu\text{-}1,2\text{-}O_2)]^{2+}$ and $[Cu_2(Me_6tren)_2(\mu\text{-}1,2\text{-}O_2)]^{2+}$, where the ν(O-O) were found to be at 825 cm^{-1} and 820 cm^{-1}, respectively. [30,38] When $^{18}O_2$ is substituted for $^{16}O_2$, the ν(O-O) peak in $[Cu_2(L^{Me})_2(\mu\text{-}1,2\text{-}O_2)]^{2+}$ is shifted to 797 cm^{-1}. This observed shift is very close to the predicted isotope shift of 795 cm^{-1}. The Cu(II)-oxygen stretch (or ν(Cu-O)) in $[Cu_2(L^{Me})_2(\mu\text{-}1,2\text{-}O_2)]^{2+}$ is observed at 543 cm^{-1} in the sample prepared from $^{16}O_2$ and shifts to 514 cm^{-1} when the sample is prepared using $^{18}O_2$. This isotopic shift is also consistent with the predicted isotope shift value of 512 cm^{-1}.

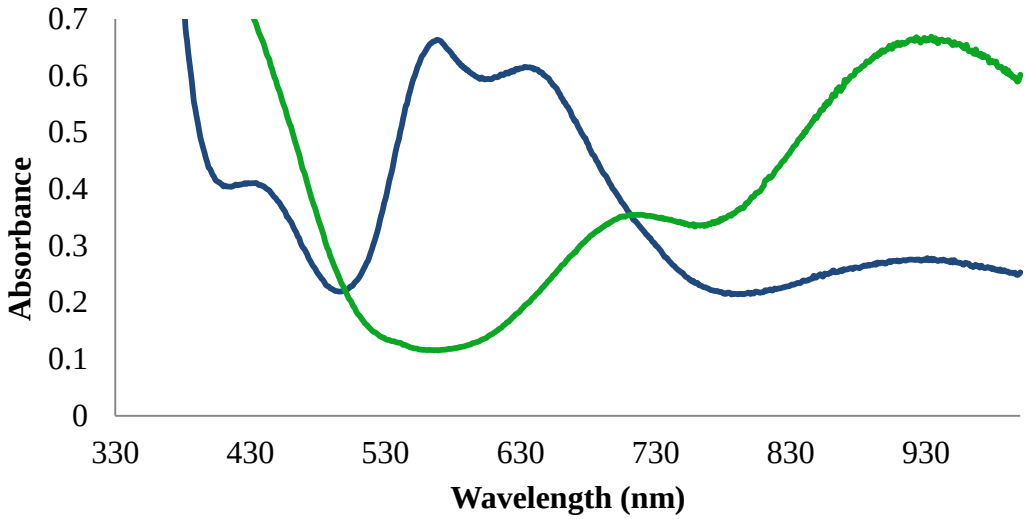

Figure 7. Decay of $[Cu_2(L^{Me})_2(O_2)](PF_6)_2$ (blue) to $[Cu(L^{Me})OH](PF_6)$ (green) in a solution of acetone with warming from 10 °C to ambient temperature. Δt=30s

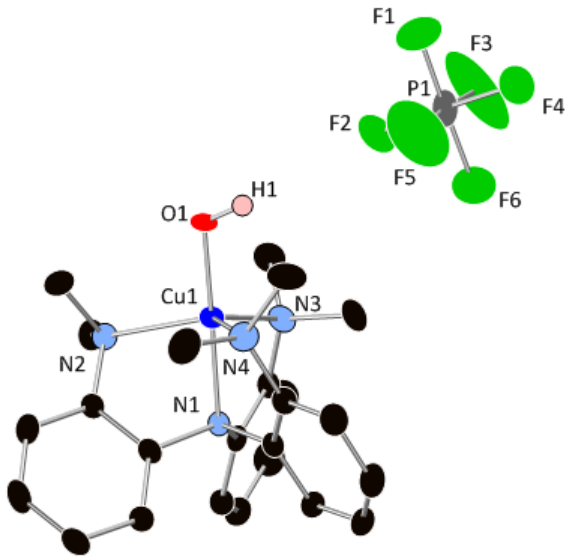

Figure 8. Crystal structure of $[Cu(L^{Me})(OH)]PF_6$. Selected bond lengths (Å) and angles (deg.): Cu1—N1 2.04(3), average Cu1—N(2,3,4) 2.12(3), Cu1—O1 1.83(2), N1—Cu1—N(2,3,4) 83.2(12), N1—Cu1—O1 178.9(12). Hydrogens are omitted for clarity except the -OH and thermal ellipsoids are shown at 50% probability.

Decay of Cu^{II}-peroxo Complexes to Cu^{II}-OH Complexes. Warming of $[Cu_2(L^{Me})_2(\mu\text{-}1,2\text{-}O_2)](PF_6)_2$ in a coordinating solvent to ambient temperature shows the formation of a new product through UV-visible absorption spectroscopy (**Figure 7**). In the spectrum, two peaks are observed at 722 nm (74.7 M^{-1} cm^{-1}) and 943 nm (56.7 M^{-1} cm^{-1}) showing an absorbance pattern characteristic of a trigonal bipyramidal copper(II) complex, similar to the pattern observed in $[Cu^{II}(L^{Me})Cl]PF_6$. X-ray quality crystals were obtained of this new complex by the diffusion of ether into a concentrated acetonitrile solution of the green product. The results of the X-ray crystallographic data confirm the formation of a monocopper hydroxide seen in **Figure 8**. Although, other groups have observed a similar decay of a dicopper(II) *trans*-μ-1,2-peroxo complex, the products isolated in their studies were characterized as a dinuclear $(\mu\text{-}OH)_2$ bridging hydroxide species. [39] The crystal structure of $[Cu^{II}(L^{Me})(OH)]PF_6$ shows a copper oxygen bond length of 1.83(2) Å, which is shorter than other reported terminal hydroxide complexes. A dicopper complex containing a terminal hydroxide ligand synthesized by Masuda and co-workers reported a Cu—OH bond length of 1.989(4) Å.[54] Mononuclear copper(II) hydroxides (**Figure 9**) characterized by Tolman and Okamoto have copper-oxygen bond lengths of 1.878(2) Å and 1.918(4) Å respectively. [55,56] This shorter copper to oxygen bond length may be attributed to the more electron withdrawing nature of the ligand L^{Me}.

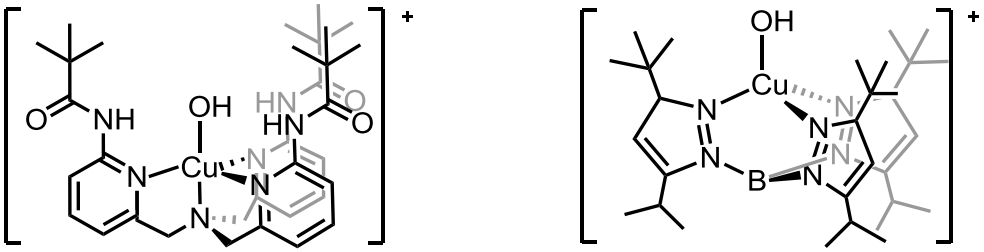

Figure 9. Examples of terminal mononuclear copper(II) hydroxide complexes found in the literature.[55,56]

Table 4. Yields of the products resulting from the oxidation of toluene by various copper-dioxygen complexes.[38]

Complex	**Benzaldehyde**	**Benzyl alcohol**
$[Cu^{II}_2(Me_6tren)_2(\mu\text{-}1,2\text{-}O_2)](BPh_4)_2$	~10%	~1%
$[Cu^{II}_2(tmpa)_2(\mu\text{-}1,2\text{-}O_2)](BPh_4)_2$	~20%	traces

Reactivity of Cu^{II}-peroxo Complexes with Toluene. The choice of ligand and counterion both play a crucial role in the reactivity of dicopper *trans*-μ-1,2-peroxo complexes. Manipulation of the ligand's field strength and electron donating ability have been thoroughly investigated in its binding to copper(I) and the complex's subsequent reactivity to dioxygen.[41,53,57] Spectroscopic studies have concluded that ligands with a stronger electron donating ability strengthened the copper(II) oxygen bond and subsequently weakened the oxygen-oxygen bond.[53,57] As previously mentioned, works by both Karlin and Schindler have shown the ability of dicopper(II) *trans*-μ-1,2-peroxo complexes to selectively oxidize toluene to benzaldehyde.[38,39,58] The ligands used in these studies, tmpa and Me_6tren, have been shown to possess different field strengths and

electron donating abilities, where Me_6tren is the stronger field ligand with a stronger electron donating ability. **Table 4** shows the results of the stoichiometric oxidation of toluene, where $[Cu^{II}_2(Me_6tren)_2(\mu\text{-}1,2\text{-}O_2)](BPh_4)_2$ demonstrates a 10% conversion of toluene to benzaldehyde with 1% benzyl alcohol produced. The exchange of the ligand for tmpa, which has a weaker field and weaker electron donating properties, improves the yield of benzaldehyde to 20% with trace amounts of benzyl alcohol present.[38] These results show that stronger field ligands are less selective and produce smaller yields of the desired product, benzaldehyde.

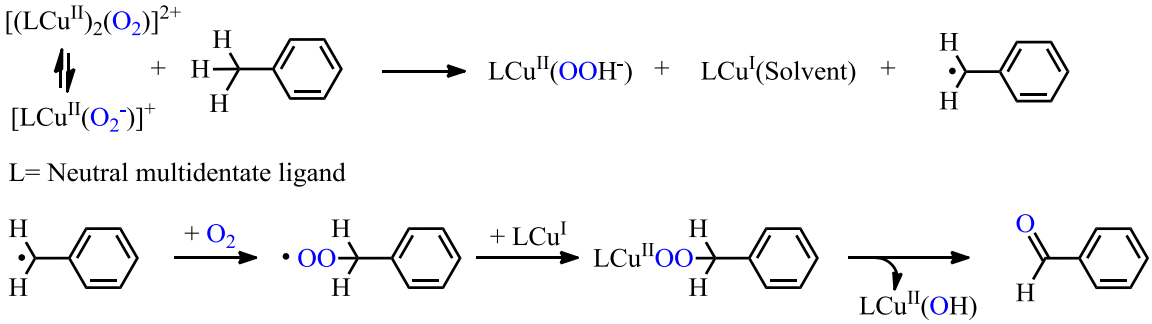

Scheme 2. One possible proposed mechanism for the oxidation of toluene to benzaldehyde using copper(II) peroxide complexes.[40]

The first stoichiometric oxidation of toluene was attempted using $[Cu^{II}_2(L^{Me})_2(\mu\text{-}1,2\text{-}O_2)](PF_6)_2$. However, this reaction could be stirred for several days with minimal conversion of toluene to its oxidized products or formation of the $[Cu^{II}(L^{Me})(OH)]PF_6$ decay product possibly due to its limited solubility. This was addressed by the use of BPh_4^- as the counterion in $[Cu^{II}_2(Me_6tren)_2(\mu\text{-}1,2\text{-}O_2)]^{2+}$ and $[Cu^{II}_2(tmpa)_2(\mu\text{-}1,2\text{-}O_2)]^{2+}$.[38,39] This large organic anion improves the solubility of the dicopper(II) *trans*-μ-1,2-peroxo complexes in nonpolar organic solvents, which is important for the initiation

of toluene oxidation. With this in mind, the oxidation of toluene was performed with $[Cu^{II}_2(L^{Me})_2(\mu\text{-}1,2\text{-}O_2)](PF_6)_2$, using two equivalents of $NaBPh_4$, resulting in an *in-situ* salt metathesis. Preliminary results show that $[Cu^{II}_2(L^{Me})_2(\mu\text{-}1,2\text{-}O_2)](PF_6)_2$ yields ~50% benzaldehyde with trace amounts of benzyl alcohol. The yields of the corresponding products were analyzed by GC. Taking into consideration that a dicopper(II) peroxide complex would most likely be a two electron oxidant and the conversion of toluene to benzaldehyde requires four electrons (**Scheme 2**), our best recorded yield is actually two times greater than the stoichiometric ~50%, which gives $[Cu^{II}_2(L^{Me})_2(\mu\text{-}1,2\text{-}O_2)](PF_6)_2$ a yield of ~100%. This conclusion fits with the trend that weak field coordinating ligands have the ability to enhance the selectivity and efficiency of dicopper(II) *trans-*μ-1,2-peroxo complexes for the production of benzaldehyde in the oxidation of toluene.

However, these preliminary results have been inexplicably irreproducible. An alternative procedure for the synthesis of the starting complex $[Cu^{I}(L^{Me})(CH_3CN)]PF_6$, which avoids the use of acetonitrile, has been applied without improvement of the results for the reactivity of $[Cu^{II}_2(L^{Me})_2(\mu\text{-}1,2\text{-}O_2)](PF_6)_2$. To better understand the technique for the oxidation of toluene, $[Cu^{I}(tmpa)(CH_3CN)]BPh_4$ and $[Cu^{II}_2(tmpa)_2(\mu\text{-}1,2\text{-}O_2)](BPh_4)_2$ were synthesized using literature procecures.[38] Yields from the reaction of $[Cu^{II}_2(tmpa)_2(\mu\text{-}1,2\text{-}O_2)](BPh_4)_2$ with toluene were found to be 11.5%, which is lower than the reported results in **Table 4**. By attempting to reproduce these literature results for the oxidation of toluene, difficulties in the isolation of $[Cu^{II}_2(tmpa)_2(\mu\text{-}1,2\text{-}O_2)](BPh_4)_2$ are observed because warming the solution to anything above ~ -75 ^{o}C results in the isolation of the green copper(II) hydroxide product. This indicates that the procedure for the isolation of $[Cu^{II}_2(L^{Me})_2(\mu\text{-}1,2\text{-}O_2)](PF_6)_2$ may need to be modified to

prevent a similar occurrence, which may be affecting the results for the oxidation of toluene.

At the end of the stoichiometric oxidation of toluene with $[Cu^{II}_2(L^{Me})_2(\mu\text{-}1,2\text{-}O_2)](PF_6)_2$, we expected to isolate the green $[Cu^{II}(L^{Me})(OH)]PF_6$ complex observed in the toluene oxidation reactions of $[Cu^{II}_2(Me_6tren)_2(\mu\text{-}1,2\text{-}O_2)](BPh_4)_2$ and $[Cu^{II}_2(tmpa)_2(\mu\text{-}1,2\text{-}O_2)](BPh_4)_2$. However, the blue $[Cu^{II}_2(L^{Me})_2(\mu\text{-}1,2\text{-}O_2)](PF_6)_2$ starting material was obtained. We believe this is due to the ability of $NaBPh_4$ to act as a one electron reducing agent.[59,60] The reaction occurs by breaking one of the B—Ph bonds to donate one electron to $[Cu^{II}(L^{Me})(OH)]PF_6$, forming copper(I). The other products include a neutral molecule of BPh_3 and a phenyl radical, which will either react with itself to form biphenyl or with a hydroxide to make phenol.[59,60] These byproduct have been observed by gas chromatograph, in the case of phenol and biphenyl, and mass spectrometry, for BPh_3.

Our studies would be the first known report of the catalytic oxidation of toluene by a dicopper(II) *trans*-μ-1,2-peroxo complex supported by a tetraamine. However, difficulties in the reproducibility of the oxidation of toluene using $[Cu^{II}_2(L^{Me})_2(\mu\text{-}1,2\text{-}O_2)](PF_6)_2$ and $NaBPh_4$ suggest this reaction is very sensitive to impurities or the radicals formed by the oxidation $NaBPh_4$. Oxidation reactions with the addition of 4 equivalents of $NaBPh_4$ compared to 2 equivalents show an increase in the yield of benzaldehyde from ~1% to ~4%. The synthesis of $[Cu^{I}(L^{Me})(CH_3CN)]PF_6$ substituting acetone over acetonitrile, a highly coordinating solvent, prevents impurities as a result in incomplete metallation or variations in the denticity of the copper(I) complex. However, this does not seem to improve the consistency of the oxidation of toluene. The reaction of

$[Cu^{II}_2(L^{Me})_2(\mu\text{-}1,2\text{-}O_2)](PF_6)_2$ and $NaBPh_4$ was then explored in the absence of toluene using acetone as the solvent. This reaction occurs overnight and the products monitored by gas chromatography reveal the production of phenol and biphenyl. If one equivalent of toluene is added to this reaction, no production of benzaldehyde is observed indicating that the competing reaction of $[Cu^{II}_2(L^{Me})_2(\mu\text{-}1,2\text{-}O_2)](PF_6)_2$ with $NaBPh_4$ is more favorable.

Reactivity of Cu^{II}-peroxo Complexes with Alternative Substrates. The oxidation of alternative substrates was explored using 2,4-*tert*-butylphenol and 9,10-dihydroanthracene because of their weaker C—H BDEs compared to toluene. This type of reactivity has been previously explored using Cu^{II}_2-η^2:η^2-peroxo and Cu^{III}_2-bis(μ-oxo) complexes.[33,61-64] Work previously reported by Stack and Tolman using these dicopper-dioxygen complexes show on separate occasions that the oxidation of 9,10-dihydroanthracene does not occur.[22,63,64] Studies exploring the reactivity of copper complexes with 2,4-*tert*-butylphenol were attempting to replicate reactivity shown by tyrosinase. However, the oxidation of 2,4-*tert*-butylphenol doesn't result in the formation of a catechol but typically of the coupled diphenol product.[33,61,63,64]

Neither of these C—H bond oxidation reactions have been reported using Cu^{II}_2-μ-1,2-peroxo complexes. Using $[Cu^{II}_2(L^{Me})_2(\mu\text{-}1,2\text{-}O_2)](PF_6)_2$ both of these reactions were performed stoichiometrically in acetone and were analyzed by gas chromatography. The spectroscopy reveals no reaction of $[Cu^{II}_2(L^{Me})_2(\mu\text{-}1,2\text{-}O_2)](PF_6)_2$ with either substrate after 3 days of stirring at room temperature. The color change of the solution to brown is attributed to further degradation of the $[Cu^{II}(L^{Me})OH]PF_6$ species, the products of which were unidentifiable using mass spectroscopy.

Since the oxidation of 9,10-dihydroanthracene is not yet predictable, very little can be concluded from these results. For the lack of reactivity of $[Cu^{II}_2(L^{Me})_2(\mu\text{-}1,2\text{-}O_2)](PF_6)_2$ with 2,4-*tert*-butylphenol, there may give some implications about the mechanism of our complex. Mechanistic studies of Cu^{II}_2-η^2:η^2-peroxo and Cu^{III}_2-bis(μ-oxo) complexes show that a proton coupled electron transfer is more favorable than direct hydrogen atom transfer.[33,61] This may suggest that direct hydrogen atom transfer mechanism is more favorable with our $[Cu^{II}_2(L^{Me})_2(\mu\text{-}1,2\text{-}O_2)](PF_6)_2$ complex, however additional experiments are required to confirm this hypothesis.

III. Conclusion

To conclude, the properties of a copper(I) complex supported by the tripodal tetraamine ligand L^{Me} was investigated. The ligand field strength of L^{Me} was explored through UV-visible spectroscopy of the halogenated complexes $[Cu^{II}(L^{Me})Cl]PF_6$, and the infrared spectroscopy of the carbonyl stretch in $[Cu^{I}(L^{Me})(CO)]PF_6$. Results show that compared to copper(I) complexes supported by other common tripodal tetraamine ligands, Me_6tren and tmpa, our ligand, L^{Me}, was the least electron donating. The ligand shows favorable metallation to a copper(I) source and the copper(I) complex was characterized by crystal structures obtained from two different counter-ions, PF_6 and OTf. The reaction of $[Cu^{I}(L^{Me})(CH_3CN)]PF_6$ with dioxygen occurred rapidly in acetone at low temperatures (-78 ^{o}C) to form a blue species that is stable as a solid. Through UV-visible absorption and resonance Raman spectroscopies the blue species was characterized as a dicopper(II) complex with a *trans*-μ-1,2-peroxo ligand, $[Cu^{II}_2(L^{Me})_2(\mu\text{-}1,2\text{-}O_2)](PF_6)_2$. If a solution of $[Cu^{II}_2(L^{Me})_2(\mu\text{-}1,2\text{-}O_2)](PF_6)_2$ in a coordinating solvent is warmed to ambient temperature, decay of the *trans*-μ-1,2-peroxide is observed and characterized as mononuclear copper(II) terminal hydroxide, $[Cu^{II}(L^{Me})(OH)]PF_6$.

Reactivity of $[Cu^{II}_2(L^{Me})_2(\mu\text{-}1,2\text{-}O_2)](PF_6)_2$ shows the selective oxidation of toluene to produce benzaldehyde in good yields with trace amounts of benzyl alcohol. However, these results are irreproducible and unpredictable. This may be attributed to the poor solubility of our complex in non-polar organic solvents and radicals formed by the addition of $NaBPh_4$ to the reaction mixture. Our complex $[Cu^{II}_2(L^{Me})_2(\mu\text{-}1,2\text{-}O_2)](PF_6)_2$ also shows no favorable reactivity with 9,10-dihydroanthracene or 2,4-*tert*-butylphenol. Other substrates that may yield more insight to the reactivity of

$[Cu^{II}_2(L^{Me})_2(\mu\text{-}1,2\text{-}O_2)](PF_6)_2$ may be tetrahydrofuoran, a more polar solvent that has shown favorable reactivity with Cu^{II}_2-η^2:η^2-peroxo complexes.[33,62] Also, to complete the study on the reactivity of $[Cu^{II}_2(L^{Me})_2(\mu\text{-}1,2\text{-}O_2)](PF_6)_2$, experiments need to be performed that better explore the change of the counterions on this species.

IV. Experimental

All reactions were performed using standard Schlenk techniques or in an MBraun Labmaster 130 drybox under an atmosphere of nitrogen. All reagents were all obtained from commercial chemical vendors and used as received, unless otherwise noted. Acetone was dried over drierite ($CaSO_4$) overnight and then distilled from fresh drierite before use. Other anhydrous solvents were purchased from Sigma-Aldrich and stored over activated sieves. Elemental analyses were performed by Atlantic Microlab, Inc., Norcoss, GA. Ambient temperature ^{1}H NMR spectra were recorded on a Varian Mercury 300 MHz spectrophotometer. Chemical shifts (δ) are reported in parts per million (ppm) and coupling constants (J) are reported in Hz. NMR spectra were referenced internally to residual solvent. Infrared spectra were recorded as KBr pellets on a Varian Scimitar 800 Series FT-IR spectrophotometer. Nujol and solution state IR spectra were recorded using the same spectrophotometer with KBr salt plates. UV-Visible absorption spectra were recorded on a Cary 50 spectrophotometer using 1.0 cm or 0.5 cm quartz cuvettes. Mass spectra were recorded in the Mass Spectrometry Center at Emory University on a JEOL JMS-SX102/SX102/A/E mass spectrometer. X-ray crystallography studies were carried out in the X-ray Crystallography Laboratory at Emory University on a Bruker Smart 1000 CCD diffractometer. Oxidation products of toluene were analyzed using a Shimadzu GC-2014 model gas chromatograph equipped with a Zebron capillary column, 30 m, I. D. 0.25 mm, and film thickness 0.25 μm. The GC conditions for the analysis of the toluene oxidation products (benzaldehyde, benzyl alcohol) were as follows. Injector port temperature, 250 °C; detector temperature, 300 °C; column temperature (initial temperature), 45 °C; initial time, 2 min; final temperature, 230 °C; final time, 10 min;

gradient rate, 25 °C/min; flow rate, 10.0 mL/min. The GC conditions for the analysis of the 2,4-*tert*butylphenol oxidation products (diphenol, catechol, and quinone) were as follows. Injector port temperature, 300 °C; detector temperature, 300 °C; column temperature (initial temperature), 150 °C; initial time, 2 min; final temperature, 300 °C; final time, 10 min; gradient rate, 35 °C/min; flow rate, 20.0 mL/min. The GC conditions for the analysis of the 9,10-dihydroanthracene oxidation products (anthracene) were as follows. Injector port temperature, 300 °C; detector temperature, 300 °C; column temperature (initial temperature), 150 °C; initial time, 2 min; final temperature, 230 °C; final time, 10 min; gradient rate, 35 °C/min; flow rate, 20.0 mL/min. $N(o\text{-}PhNH_2)_3$ and $N(o\text{-}PhNMe_2)_3$ (L^{Me}) were synthesized using published literature methods.[41,43]

Preparation of tris(2-dimethylaminophenyl)amine (L^{Me}).[41] An aqueous HCHO solution (37 w.%) (6.61 ml, 88.0 mmol) was added to an CH_3CN (100 ml) solution of $N(o\text{-}PhNH_2)_3$ (0.7993 g, 2.75 mmol) and stirred. After 15 minutes, $NaBH_3CN$ (1.6510 g, 26.3 mmol) was added to the solution as a solid. Once all of the $NaBH_3CN$ was dissolved, concentrated HOAc (0.6 ml) was added drop-wise to adjust the pH to ~4 and the reaction mixture was stirred for 12 hrs. All volatiles were then removed under reduced pressure to yield a sticky, off-white solid. A KOH solution (2 M, 50 ml) was added to the crude solid and Et_2O (3 x 20 ml) was used to extract the product. The organic layer were combined and washed with KOH solution (0.5 M, 50 ml). The organic layer was then extracted with an aqueous HCl solution (1 M, 3 x 15 ml). The aqueous extracts were combined and neutralized using solid KOH. The product was then extracted using Et_2O (3 x 20 ml). The organic layers were combined and dried over K_2CO_3. The filtrate was concentrated to dryness using a rotary evaporator to yield a light pink solid. The light pink solid was

recrystallized from hot methanol to yield the product as off-white needles (77%, 0.7959 g). ^{1}H NMR ($CDCl_3$): 7.05 (dd, 3H, *J*=1.8, *J*=7.5), 6.98 (td, 3H, *J*=1.8, *J*=6.9), 6.86 (td, 3H, *J*=1.8, *J*=7.8), 6.78 (dd, 3H, *J*=1.8, *J*=7.8), 2.39 (s, 18H). HRMS (ESI): $C_{24}H_{30}N_4$ m/z Calcd. 374.24705 Found 375.25461 $[M+1]^+$. FTIR (KBr) ν_{CO} (cm^{-1}): 3054, 2971, 2910, 2820, 2774, 1922, 1889, 1804, 1781; 1586, 1491, 1448, 1314, 1258, 954, 753.

Preparation of $[Cu^{I}(L^{Me})(CH_3CN)]PF_6$. A) A solution of $[Cu(CH_3CN)_4]PF_6$ (0.0754 g, 0.2023 mmol) in 3 mL of acetonitrile was added dropwise to a solution of L^{Me} (0.0786 g, 0.2099 mmol) in 3 mL of acetonitrile. The reaction was stirred at room temperature overnight. The solvent was removed under reduced pressure to afford a white powder. The powder was washed with Et_2O and dried on a sintered glass frit (0.1058 g, 0.1815 mmol, 89.7%). Colorless crystals were grown by diffusing Et_2O into an acetone solution. **B)** A solution of $[Cu(CH_3CN)_4]PF_6$ (0.0967 g, 0.259 mmol) in 2 mL of acetone was added slowly dropwise to a vigorously stirring solution of L^{Me} (0.1063 g, 0.284 mmol) in 1 mL of acetone over a period of 10 minutes. The solution is left to stir for 5 minutes. Et_2O (15 mL) was added dropwise to the solution with stirring until a precipitate forms and left to stir for 5 minutes. The precipitate is filtered on a sintered glass frit, washed with Et_2O (5 mL), and dried for 2 hours. (145.9 mg, 90.1%). Colorless crystals were grown by diffusing Et_2O into an acetone solution. ^{1}H NMR (300 MHz, CD_3CN): 7.10 (3H), 7.00 (3H), 6.88 (3H), 6.70 (3H), 2.37 (18H). FTIR (KBr) ν_{CO} (cm^{-1}): 3059, 2932, 2821, 2775, 1492, 1448, 1261, 1225, 1099, 1048, 841, 771, 558. MS (EM-ESI): $[Cu(L^{Me})]^+$ m/z Calcd. 437.17665. Found 437.17560 (^{63}Cu, 100), 439.17413 (^{65}Cu, 44.33).

Preparation of $Cu^{I}(L^{Me})(OTf)$. A solution of $[Cu^{I}(CH_3CN)_4]OTf$ (105 mg, 0.279 mmol) in 2 mL of acetone was added dropwise to a solution of L^{Me} (113 mg, 0.303 mmol) in 2 mL of acetone. The reaction was stirred overnight at room temperature. Et_2O (20 mL) was added to the solution with stirring until a precipitate forms. The precipitate is filtered on a sintered glass frit, washed with Et_2O (5 mL), and dried. (141 mg, 80.4%). Light yellow crystals were grown by diffusing Et_2O into an acetone solution. ^1H NMR (300 MHz, $(CD_3)_2CO$): 7.94 (6H), 7.65 (6H), 2.33 (18H). FTIR (KBr) ν_{CO} (cm^{-1}): 3070, 2961, 2873, 2834, 2785, 1493, 1447, 1275, 1224, 1151, 1105, 1030, 931, 770, 638, 580, 558, 517, 476. Anal. Calcd ($C_{50}H_{60}Cu_2F_6N_8O_8S_2$): C, 49.78; H, 5.01; N, 9.29. Found: C, 49.85; H, 5.06; N, 9.23.

Preparation of $[Cu^{I}(tmpa)(CH_3CN)]BPh_4$.[38] A solution of $[Cu(CH_3CN)_4]PF_6$ (0.107 g, 0.294 mmol) in 2 mL of acetone was added slowly dropwise to a vigorously stirring solution of tmpa (0.0922 g, 0.318 mmol) in 1 mL of acetone over a period of 10 minutes. The solution color changes to a darker yellow and it is left to stir for 5 minutes. A solution of $NaBPh_4$ (0.0986 g, 0.288 mmol) was added dropwise to the solution mixture and the solution is left to stir for 5 minutes. Et_2O (15 mL) was added dropwise to the solution with stirring until a precipitate forms and left to stir for 5 minutes. The precipitate is filtered on a sintered glass frit, washed with Et_2O (5 mL), and dried for 2 hours. (145.9 mg, 90.1%). ^1H NMR (300 MHz, CD_3CN): 7.10 (3H), 7.00 (3H), 6.88 (3H), 6.70 (3H), 2.37 (18H).

Preparation of $[Cu^{II}_2(L^{Me})_2(\mu\text{-}1,2\text{-}O_2)](PF_6)_2$. Into approximately 3 mL of acetone, $[Cu(L^{Me})(CH_3CN)]PF_6$ (67.4 mg, 0.108 mmol) was dissolved. The solution was put into a 50 mL schlenk flask and sealed with a septum. The flask was removed from

the inert atmosphere and cooled in an acetone/dry ice bath to -78^{o}C for about 10 minutes. The dry O_2(g) was then added to the head space of the flask, rapidly changing the color of the solution to blue. The reaction was left to sit for approximately 10 minutes before anhydrous Et_2O was added to the actetone solution to precipitate out the blue species. The blue powder was filtered into a sintered glass frit and dried. (54.8 mg, 0.0457 mmol, 84.7% yield). UV-vis: (acetone, -75 ^{o}C) 564 nm (3681.2 M^{-1} cm^{-1}), 614 nm (2991.4 M^{-1} cm^{-1}). FTIR (KBr) ν_{CO} (cm^{-1}): 2927, 1492, 1449, 1262, 1192, 1155, 1098, 1050, 1013, 924, 842, 784, 669, 620, 586, 559, 484.

Preparation of $[Cu^{II}_2(L^{Me})_2(\mu\text{-}1,2\text{-}O_2)](OTf)_2$. Into about 3 mL of acetone, the precursor $Cu(L^{Me})(OTf)$ (135 mg, 0.215 mmol) was dissolved in a 50 mL schlenk flask. The flask was removed from the inert atmosphere and cooled in an acetone/dry ice bath to -78 ^{o}C for about 10 minutes. The dry O_2(g) was then added to the head space of the flask, almost instantly turning the color of the solution to blue. The reaction was left to sit for approximately 10 minutes before anhydrous Et_2O was added to the acetone solution to precipitate out the blue species. The blue powder was filtered into a sintered glass frit and dried. (54.8 mg, 0.0457 mmol, 84.7% yield). UV-vis: (acetone, 10^{o}C) 453 nm (251.8 $M^{-1}cm^{-1}$), 567 nm (1021.7 $M^{-1}cm^{-1}$), 634 nm (835.9 $M^{-1}cm^{-1}$). FTIR (KBr) ν_{CO} (cm^{-1}): 3443, 2927, 1499, 1274, 1156, 1093, 1029, 911, 783, 680, 638, 483.3.

Preparation of $[Cu^{II}_2(tmpa)_2(\mu\text{-}1,2\text{-}O_2)](BPh_4)_2$.[38] Into approximately 3 mL of acetone, $[Cu^{I}(tmpa)(CH_3CN)]BPh_4$ (0.0759 g, 0.106 mmol) was dissolved. The solution was put into a 50 mL schlenk flask and sealed with a septum. The flask was removed from the inert atmosphere and cooled in an acetone/dry ice bath to -78^{o}C for about 10 minutes. The dry O_2(g) was then added to the head space of the flask, rapidly changing

the color of the solution to blue. The reaction was left to sit for approximately 10 minutes before anhydrous hexane was added to the acetone solution to precipitate out the blue species. Since hexane is not miscible with acetone at -78 ^{o}C, the flask was warmed for 5 minutes before filitering the blue powder into a sintered glass frit and dried for 2 hours. (0.0534 g, 0.0388 mmol, 73.0% yield). UV-vis: (acetone, -75 ^{o}C) 520 nm (3945.0 $M^{-1}cm^{-1}$), 592 nm (2740.6 $M^{-1}cm^{-1}$).

Preparation of [Cu(L^{Me})(OH)]PF_6. Into 6 mL of acetonitrile, [Cu(L^{Me})(CH_3CN)]PF_6 (222.2 mg, 0.356 mmol) was dissolved. This solution was left to sit at room temperature, exposed to air for 2 days. The solution color changes to green and ~30 mL of anhydrous ether was added to the flask to precipitate out the green species. The green powder was filtered into a sintered glass frit and dried. The solid was dissolved in acetonitrile and filtered through a celite plug to remove a black precipitate (CuO) before recrystallization by diffusing ether into the solution. UV-vis: (acetone, 10 ^{o}C) 722 nm (74.7 $M^{-1}cm^{-1}$), 943 nm (56.7 $M^{-1}cm^{-1}$). FTIR (KBr) ν_{CO} (cm^{-1}): 3442, 2970, 2927, 1492, 1460, 1272, 1197, 1160, 1100, 1050, 1020, 928, 839, 772, 620, 587, 558, 518, 475.

Toluene Oxidation Reaction. Into a 10 mL round bottom flask, [Cu^{II}_2(L^{Me})$_2$(μ-1,2-O_2)](PF_6)$_2$ (85.2 mg, 0.071 mmol) and $NaBPh_4$ (47.1 mg, 0.138 mmol) were added. The flask was sparged with dry O_2(g) at ambient temperature for 10 minutes. Toluene (3.0 mL, 28.2 mmol) was added and the contents are stirred overnight. The reaction was filtered through a celite plug and monitored by gas chromatography. (benzaldehyde, 49.3% yield; benzyl alcohol, <0.1%).

2,4-*tert*Butylphenol Reaction. Into a 10 mL round bottom flask, $[Cu^{I}(L^{Me})(CH_3CN)]PF_6$ (51.3 mg, 0.0823 mmol) was dissolved into 2.0 mL of a solution of 2,4-*tert*butylphenol (0.457 M, .0913 mmol) in acetone. The flask was removed from the inert atmosphere and cooled in an acetone/dry ice bath to -78^{o}C for about 10 minutes. The flask was sparged with dry O_2(g) for 10 minutes. The contents were stirred for approximately 3 days before a color change took place from blue to brown. The reaction was filtered through a celite plug, removing very little precipitate, and monitored by gas chromatography.

9,10-Dihyroanthracene Reaction. Into a 10 mL round bottom flask, $[Cu^{I}(L^{Me})(CH_3CN)]PF_6$ (50.4 mg, 0.0808 mmol) was dissolved into 2.0 mL of a solution of 9,10-dihydroanthracene (0.0424 M, 0.0848 mmol) in acetone. The flask was removed from the inert atmosphere and cooled in an acetone/dry ice bath to -78^{o}C for about 10 minutes. The flask was sparged with dry O_2(g) for 10 minutes. The contents were stirred for approximately 3 days before a color change took place from blue to brown. The reaction was filtered through a celite plug, removing very little precipitate, and monitored by gas chromatography.

V. Crystallographic Data

Table 5. Crystal data and structure refinement for $[Cu(L^{Me})(CH_3CN)]PF_6$

Empirical formula	$C_{26}H_{33}N_5F_6PCu$
Formula weight	626.08
Temperature/K	173.18 (2)
Crystal system	monoclinic
Space group	C2/c
a/Å	20.3914(17)
b/Å	14.5398(12)
c/Å	22.947(3)
α/°	90.00
β/°	115.8010(10)
γ/°	90.00
Volume/Å^3	6125.3(10)
Z	8
Crystal size/mm^3	0.378 × 0.204 × 0.201
Reflections collected	46460
Independent reflections	6368[R(int) = 0.0549]
Data/restraints/parameters	6368/0/372
Goodness-of-fit on F^2	0.845
Final R indexes [I>=2σ (I)]	R_1 = 0.0480, wR_2 = 0.1615
Final R indexes [all data]	R_1 = 0.0630, wR_2 = 0.1860
Largest diff. peak/hole / e Å^{-3}	1.029/-0.581

Table 6. Crystal data and structure refinement for $Cu^{I}(L^{Me})(OTf)$.

Empirical formula	$C_{25}H_{30}N_4O_3F_3SCu$
Formula weight	587.13
Temperature/K	173.2 (2)
Crystal system	monoclinic
Space group	$P2_1/n$
a/Å	8.7711(18)
b/Å	20.367(4)
c/Å	14.856(3)
α/°	90.00
β/°	99.76(3)
γ/°	90.00
Volume/$Å^3$	2615.5(9)
Z	4
Crystal size/mm^3	0.265 × 0.386 × 0.426
Reflections collected	33176
Independent reflections	4815[R(int) = 0.0246]
Data/restraints/parameters	4815/0/454
Goodness-of-fit on F^2	1.029
Final R indexes [I>=2σ (I)]	R_1 = 0.0446, wR_2 = 0.1296
Final R indexes [all data]	R_1 = 0.0460, wR_2 = 0.1312
Largest diff. peak/hole / e $Å^{-3}$	0.81/-0.98

Table 7. Crystal data and structure refinement for $[Cu(L^{Me})OH]PF_6$.

Empirical formula	$C_{24}H_{31}CuF_6N_4OP$
Formula weight	600.04
Temperature/K	173.2 (2)
Crystal system	monoclinic
Space group	$P2_1/c$
a/Å	8.2191(7)
b/Å	12.9883(12)
c/Å	23.549(2)
α/°	90.00
β/°	99.1850(10)
γ/°	90.00
Volume/Å^3	2481.6(4)
Z	4
Crystal size/mm^3	0.32 × 0.27 × 0.1
Reflections collected	49106
Independent reflections	7549[R(int) = 0.0869]
Data/restraints/parameters	7549/0/334
Goodness-of-fit on F^2	1.017
Final R indexes [I>=2σ (I)]	R_1 = 0.0692, wR_2 = 0.1756
Final R indexes [all data]	R_1 = 0.1213, wR_2 = 0.2077
Largest diff. peak/hole / e Å^{-3}	1.142/-0.805

Acknowledgements

Research advisor: Cora E. MacBeth, Ph.D.

Committee members: Karl Hagen, Ph.D.; Christopher Scarborough, Ph.D.

Group members: Kelly Kluge, Ph.D.; Omar Villanueva, Neha Ahjuma

Former group members: Matthew B. Jones, Ph.D.; Lei Chu

Bryant Chica and Brian Dyer, Ph.D. for resonance Raman spectroscopy data

Kenneth I. Hardcastle, Ph.D.; John Bacsa, Ph.D.; Kelly A. Kluge, Ph.D. for X-ray crystallographic assistance

Frederick H. Strobel, Ph.D.; Elizabeth Magnotti of Mass Spectroscopy Center

VI. References

(1) Company, A.; Yao, S.; Ray, K.; Driess, M. *Chem. Eur. J.* **2010**, *16*, 9669.

(2) Dash, S.; Patel, S.; Mishra, B. K. *Tetrahedron* **2009**, *65*, 707.

(3) Punniyamurthy, T.; Velusamy, S.; Iqbal, J. *Chem. Rev.* **2005**, *105*, 2329.

(4) Cornell, C. N.; Sigman, M. S. *Inorg. Chem.* **2007**, *46*, 1903.

(5) Gamez, P.; Aubel, P. G.; Driessen, W. L.; Reedijk, J. *Chem. Soc. Rev.* **2001**, *30*, 376.

(6) Balasubramanian, R.; Rosenzweig, A. C. *Acc. Chem. Res.* **2007**, *40*, 573.

(7) Klinman, J. P. *J. Biol. Chem.* **2006**, *281*, 3013.

(8) Himes, R. A.; Karlin, K. D. *Curr. Opin. Chem. Biol.* **2009**, *13*, 119.

(9) Himes, R. A.; Barnese, K.; Karlin, K. D. *Angew. Chem., Int. Ed.* **2010**, *49*, 6714.

(10) Lieberman, R. L.; Rosenzweig, A. C. *Nature* **2005**, *434*, 177.

(11) Blain, I.; Slama, P.; Giorgi, M.; Tron, T.; Reglier, M. *Rev. Mol. Biotechnol.* **2002**, *90*, 95.

(12) Zhang, C. X.; Liang, H.-C.; Humphreys, K. J.; Karlin, K. D. *Catal. Met. Complexes* **2003**, *26*, 79.

(13) Poater, A.; Cavallo, L. *Inorg. Chem.* **2009**, *48*, 4062.

(14) Donoghue, P. J.; Gupta, A. K.; Boyce, D. W.; Cramer, C. J.; Tolman, W. B. *J. Am. Chem. Soc.* **2010**, *132*, 15869.

(15) Fujisawa, K.; Tanaka, M.; Moro-oka, Y.; Kitajima, N. *J. Am. Chem. Soc.* **1994**, *116*, 12079.

(16) Woertink, J. S.; Tian, L.; Maiti, D.; Lucas, H. R.; Himes, R. A.; Karlin, K. D.; Neese, F.; Wurtele, C.; Holthausen, M. C.; Bill, E.; Sundermeyer, J.; Schindler, S.; Solomon, E. I. *Inorg. Chem.* **2010**, *49*, 9450.

(17) Chen, P.; Root, D. E.; Campochiaro, C.; Fujisawa, K.; Solomon, E. I. *J. Am. Chem. Soc.* **2003**, *125*, 466.

(18) Askari, M. S.; Girard, B.; Murugesu, M.; Ottenwaelder, X. *Chem. Commun.* **2011**, *47*, 8055.

(19) Reynolds, A. M.; Gherman, B. F.; Cramer, C. J.; Tolman, W. B. *Inorg. Chem.* **2005**, *44*, 6989.

(20) Cramer, C. J.; Tolman, W. B. *Acc. Chem. Res.* **2007**, *40*, 601.

(21) Aboelella, N. W.; Lewis, E. A.; Reynolds, A. M.; Brennessel, W. W.; Cramer, C. J.; Tolman, W. B. *J. Am. Chem. Soc.* **2002**, *124*, 10660.

(22) Hatcher, L. Q.; Karlin, K. D. *Adv. Inorg. Chem.* **2006**, *58*, 131.

(23) Prigge, S. T.; Eipper, B. A.; Mains, R. E.; Amzel, L. M. *Science* **2004**, *304*, 864.

(24) Prigge, S. T.; Kolhekar, A. S.; Eipper, B. A.; Mains, R. E.; Amzel, L. M. *Science* **1997**, *278*, 1300.

(25) Zhang, C. X.; Kaderli, S.; Costas, M.; Kim, E.-i.; Neuhold, Y.-M.; Karlin, K. D.; Zuberbuehler, A. D. *Inorg. Chem.* **2003**, *42*, 1807.

(26) Maiti, D.; Woertink, J. S.; Narducci Sarjeant, A. A.; Solomon, E. I.; Karlin, K. D. *Inorg. Chem.* **2008**, *47*, 3787.

(27) Schatz, M.; Becker, M.; Thaler, F.; Hampel, F.; Schindler, S.; Jacobson, R. R.; Tyeklar, Z.; Murthy, N. N.; Ghosh, P.; Chen, Q.; Zubieta, J.; Karlin, K. D. *Inorg. Chem.* **2001**, *40*, 2312.

(28) Becker, M.; Heinemann, F. W.; Schindler, S. *Chem. Eur. J.* **1999**, *5*, 3124.

(29) Weitzer, M.; Schindler, S.; Brehm, G.; Schneider, S.; Hoermann, E.; Jung, B.; Kaderli, S.; Zuberbuehler, A. D. *Inorg. Chem.* **2003**, *42*, 1800.

(30) Mirica, L. M.; Ottenwaelder, X.; Stack, T. D. P. *Chem. Rev.* **2004**, *104*, 1013.

(31) Tabuchi, K.; Ertem, M. Z.; Sugimoto, H.; Kunishita, A.; Tano, T.; Fujieda, N.; Cramer, C. J.; Itoh, S. *Inorg. Chem.* **2011**, *50*, 1633.

(32) Shearer, J.; Zhang, C. X.; Hatcher, L. Q.; Karlin, K. D. *J. Am. Chem. Soc.* **2003**, *125*, 12670.

(33) Shearer, J.; Zhang, C. X.; Zakharov, L. N.; Rheingold, A. L.; Karlin, K. D. *J. Am. Chem. Soc.* **2005**, *127*, 5469.

(34) Mirica, L. M.; Vance, M.; Rudd, D. J.; Hedman, B.; Hodgson, K. O.; Solomon, E. I.; Stack, T. D. P. *Science* **2005**, *308*, 1890.

(35) Citek, C.; Lyons, C. T.; Wasinger, E. C.; Stack, T. D. P. *Nat. Chem.* **2012**, *4*, 317.

(36) Tahsini, L.; Kotani, H.; Lee, Y.-M.; Cho, J.; Nam, W.; Karlin, K. D.; Fukuzumi, S. *Chem. Eur. J.* **2012**, *18*, 1084.

(37) Fukuzumi, S.; Kotani, H.; Lucas, H. R.; Doi, K.; Suenobu, T.; Peterson, R. L.; Karlin, K. D. *J. Am. Chem. Soc.* **2010**, *132*, 6874.

(38) Wuertele, C.; Sander, O.; Lutz, V.; Waitz, T.; Tuczek, F.; Schindler, S. *J. Am. Chem. Soc.* **2009**, *131*, 7544.

(39) Lucas, H. R.; Li, L.; Narducci Sarjeant, A. A.; Vance, M. A.; Solomon, E. I.; Karlin, K. D. *J. Am. Chem. Soc.* **2009**, *131*, 3230.

(40) Schindler, S. *Eur. J. Inorg. Chem.* **2000**, *2000*, 2311.

(41) Chu, L.; Hardcastle, K. I.; MacBeth, C. E. *Inorg. Chem.* **2010**, *49*, 7521.

(42) Jones, M. B.; MacBeth, C. E. *Inorg. Chem.* **2007**, *46*, 8117.

(43) Jones, M. B.; Hardcastle, K. I.; MacBeth, C. E. *Polyhedron* **2010**, *29*, 116.

(44) Komiyama, K.; Furutachi, H.; Nagatomo, S.; Hashimoto, A.; Hayashi, H.; Fujinami, S.; Suzuki, M.; Kitagawa, T. *Bull. Chem. Soc. Jpn.* **2004**, *77*, 59.

(45) Karlin, K. D.; Hayes, J. C.; Juen, S.; Hutchinson, J. P.; Zubieta, J. *Inorg. Chem.* **1982**, *21*, 4106.

(46) Fry, H. C.; Lucas, H. R.; Narducci Sarjeant, A. A.; Karlin, K. D.; Meyer, G. J. *Inorg. Chem.* **2008**, *47*, 241.

(47) Kretzer, R. M.; Ghiladi, R. A.; Lebeau, E. L.; Liang, H.-C.; Karlin, K. D. *Inorg. Chem.* **2003**, *42*, 3016.

(48) Ferguson, G.; Parvez, M. *Acta Crystallogr., Sect. B* **1979**, *B35*, 2207.

(49) Kimura, E.; Koike, T.; Kodama, M.; Meyerstein, D. *Inorg. Chem.* **1989**, *28*, 2998.

(50) Achternbosch, M.; Apfel, J.; Fuchs, R.; Kluefers, P.; Selle, A. *Z Anor. Allg. Chem.* **1996**, *622*, 1365.

(51) Kujime, M.; Kurahashi, T.; Tomura, M.; Fujii, H. *Inorg. Chem.* **2006**, *46*, 541.

(52) Connelly, N. G.; Geiger, W. E. *Chem. Rev.* **1996**, *96*, 877.

(53) Henson, M. J.; Vance, M. A.; Zhang, C. X.; Liang, H.-C.; Karlin, K. D.; Solomon, E. I. *J. Am. Chem. Soc.* **2003**, *125*, 5186.

(54) Arii, H.; Funahashi, Y.; Jitsukawa, K.; Masuda, H. *Dalton Trans.* **2003**, 2115.

(55) Berreau, L. M.; Mahapatra, S.; Halfen, J. A.; Young, V. G., Jr.; Tolman, W. B. *Inorg. Chem.* **1996**, *35*, 6339.

(56) Fujisawa, K.; Kobayashi, T.; Fujita, K.; Kitajima, N.; Moro-oka, Y.; Miyashita, Y.; Yamada, Y.; Okamoto, K. *Bull. Chem. Soc. Jpn.* **2000**, *73*, 1797.

(57) Zhang, C. X.; Kaderli, S.; Costas, M.; Kim, E.-i.; Neuhold, Y.-M.; Karlin, K. D.; Zuberbuehler, A. D. *Inorg. Chem.* **2003**, *42*, 1807.

(58) Maiti, D.; Woertink Julia, S.; Narducci Sarjeant Amy, A.; Solomon Edward, I.; Karlin Kenneth, D. *Inorg. Chem.* **2008**, *47*, 3787.

(59) Martinho, M.; Blain, G.; Banse, F. *Dalton Trans.* **2010**, *39*, 1630.

(60) Thibon, A.; England, J.; Martinho, M.; Young, V. G.; Frisch, J. R.; Guillot, R.; Girerd, J.-J.; Muenck, E.; Que, L., Jr.; Banse, F. *Angew. Chem., Int. Ed.* **2008**, *47*, 7064.

(61) Osako, T.; Ohkubo, K.; Taki, M.; Tachi, Y.; Fukuzumi, S.; Itoh, S. *J. Am. Chem. Soc.* **2003**, *125*, 11027.

(62) Zhang, C. X.; Liang, H.-C.; Kim, E.-i.; Shearer, J.; Helton, M. E.; Kim, E.; Kaderli, S.; Incarvito, C. D.; Zuberbühler, A. D.; Rheingold, A. L.; Karlin, K. D. *J. Am. Chem. Soc.* **2002**, *125*, 634.

(63) Mahadevan, V.; DuBois, J. L.; Hedman, B.; Hodgson, K. O.; Stack, T. D. P. *J. Am. Chem. Soc.* **1999**, *121*, 5583.

(64) York, J. T.; Llobet, A.; Cramer, C. J.; Tolman, W. B. *J. Am. Chem. Soc.* **2007**, *129*, 7990.